Electronic Supplementary Material (ESI) for Journal of Materials Chemistry A.

Supporting information

Synthesis of nano-porous carbon and nitrogen doped carbon dots from an anionic MOF: A trace cobalt metal residue in carbon dots promotes electrocatalytic ORR activity

Sohini Bhattacharyya[a],[†] Bharathi Konkena[b],[†] Kolleboyina Jayaramulu[a], Wolfgang Schuhmann[b]* and Tapas Kumar Maji[a]*

[a] Molecular Materials Laboratory, Chemistry and Physics of Materials Unit, Jawaharlal Nehru Centre for Advanced Scientific Research, Jakkur, Bangalore, India
E-mail: tmaji@jncasr.ac.in

[b] Analytical Chemistry - Centre for Electrochemical Sciences (CES), Ruhr-University Bochum, Universitätsstr. 150, D-44780 Bochum, Germany

[†] Both authors have contributed equally to this work.

Synthesis of $\{[Mg_3(ndc)_{2.5}(HCO_2)_2(H_2O)]\cdot[NH_2Me_2]\cdot 2H_2O\cdot DMF\}$ (1)

The compound **1** is synthesized by a solvothermal reaction between 1,4-naphthalene dicarboxylic acid (ndc) and $MgNO_3.6H_2O$ in a dimethylformamide (DMF) medium at 120°C by a previously reported procedure.[10]

Preparation of Sample for Adsorption Measurement:

Adsorption isotherms of CO_2 at 195 K, 273 K and 298 K and N_2 at 77 K were recorded with the dehydrated sample using QUANTACHROME QUADRASORB-SI analyzer. To prepare the dehydrated sample of **NPC-1** and **NCD-1** approximately 100 mg of sample was taken in a sample holder and degassed at 160°C at 10^{-1} Pa vacuum for about 12 h prior to measurements. The dead volume of the sample cell was measured using He of 99.999% purity. The amount of adsorbed gas was calculated from the pressure difference ($P_{cal} - P_e$), where P_{cal} is the calculated pressure with no gas adsorption and P_{e} is the observed equilibrium pressure. All operations were computer-controlled and automatic.

Figures and Tables:

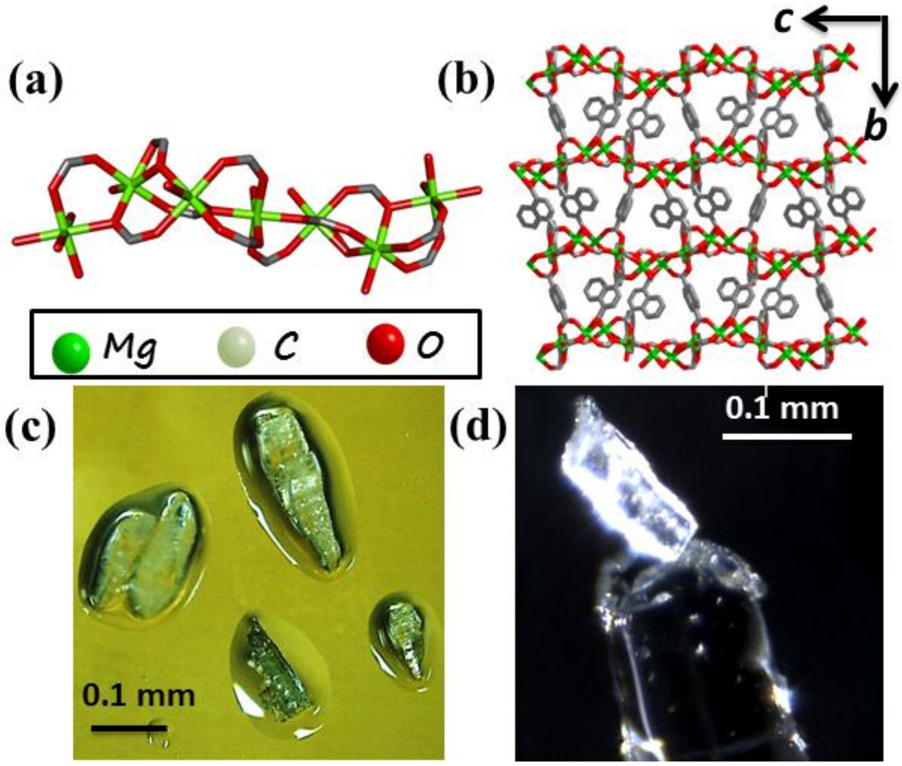

Fig. S1 (a) View of the 1D chain $Mg_3(\mu\text{-}COO)_{2.5}(\mu\text{-}OCO)_2$ of **1** along the *a* direction, **(b)** 3D networks of **1** in the *a* direction, **(c)** Photograph of the **s**ingle crystals of **1** under the microscope, **(d)** Single crystal of **1** mounted on a glass fibre for X-ray diffraction.

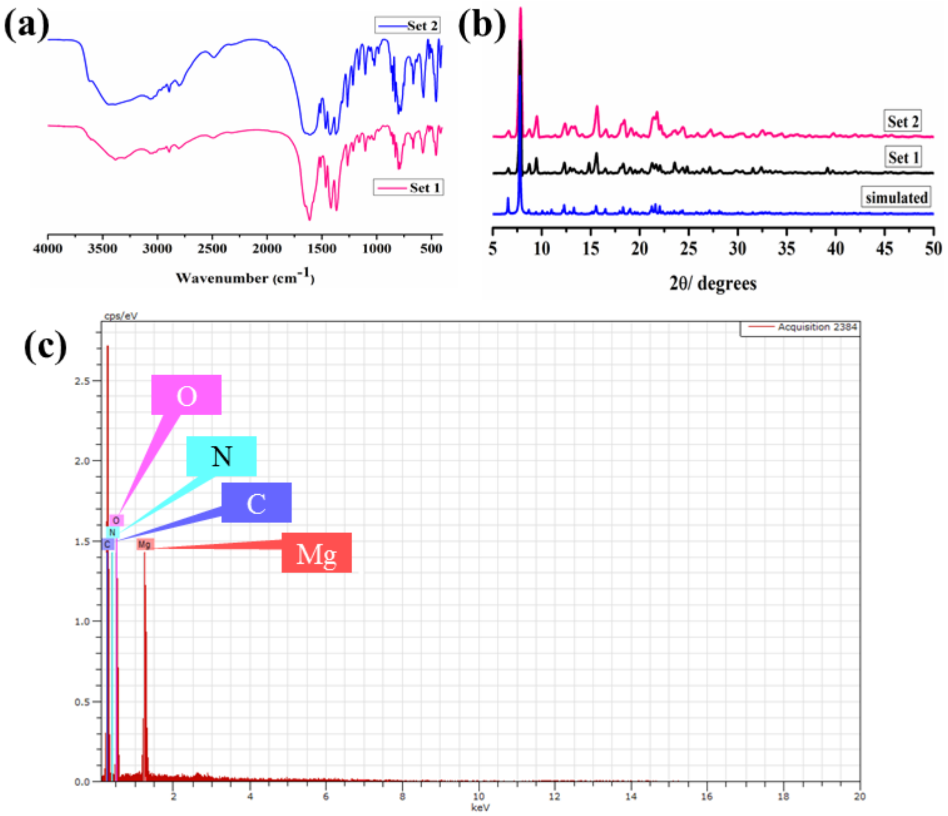

Fig. S2 (a) FTIR spectrum for two different batches of **1**, **(b)** PXRD patterns of two batches of **1** synthesized for the preparation of NCD-1 and NPC-1, **(c)** EDX analysis showing the presence of Mg, N, C and O in **1**.

Table S1 Principal peaks in the IR spectrum of **1** (**Fig. S2(a)**).

Peak Position	**Nature**	**Vibration**
1269, 1374cm^{-1}	Strong	C-N stretch
1640cm^{-1}	Strong	C=O stretch
795cm^{-1}	Strong	Aromatic C-H stretch
2809, 3063cm^{-1}	strong, broad	N-H stretch

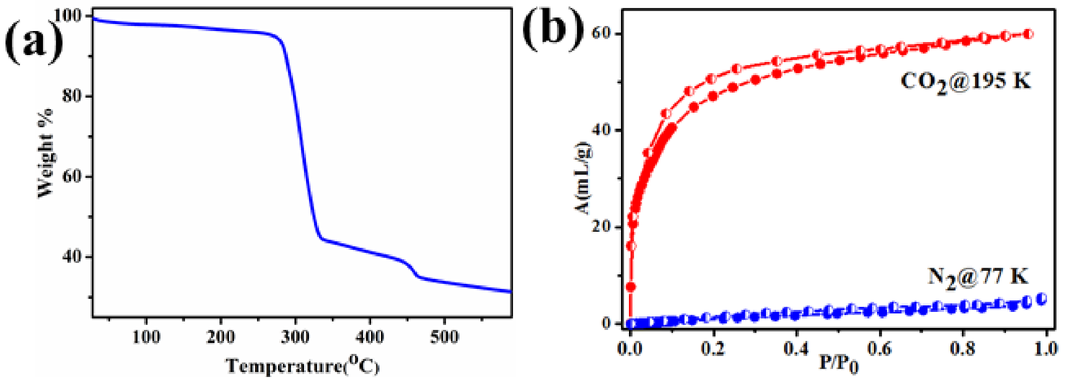

Fig. S3 (a) TGA profile of **1**, **(b)** CO_2 adsorption isotherm at 195 K and N_2 adsorption isotherm at 77 K for **1**.

TGA of 1

The initial ~6% weight loss till 100°C in **1** can be attributed to the loss of one coordinated water and two guest water molecules. The next ~ 8% weight loss till 170°C corresponds to the loss of one DMF molecule. Beyond this the framework decomposes continuously.[10]

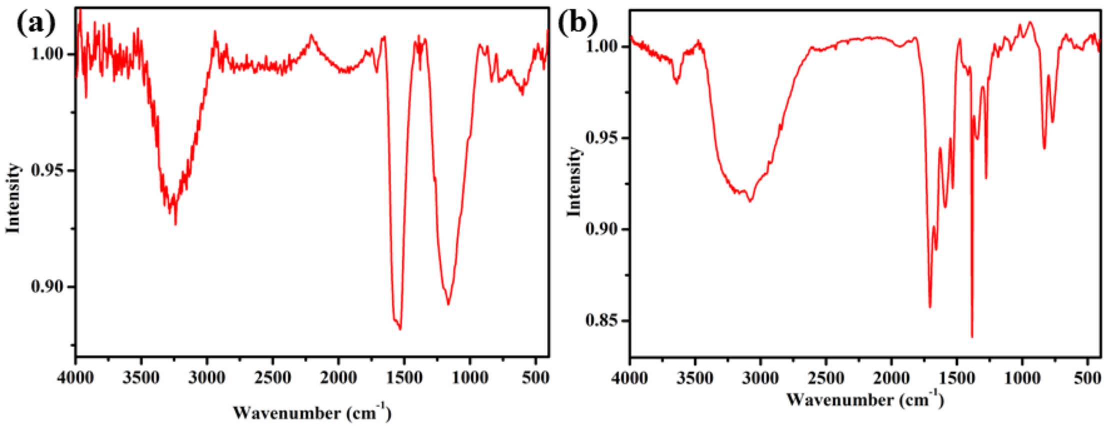

Fig. S4 IR spectra of **(a) NPC-1** and **(b) NCD-1.**

Table S2 Principal peaks in the IR spectrum of **NPC-1** (**Fig. S4(a)**).

Peak Position (cm^{-1})	**Nature**	**Vibration**
1160	Strong	C-O stretch
1385	weak, sharp	C-H rock
1550	Strong	Aromatic C-C stretch
1715	weak, sharp	C=O stretch
3290	broad, strong	O-H stretch

Table S3 Principal peaks in the IR spectrum of **NCD-1** (**Fig. S4(b)**).

Peak Position (cm^{-1})	**Nature**	**Vibration**
826	short, sharp	Breathing mode for *s*-triazine ring system
1280	short, sharp	C-N stretch
1528	short, sharp	N-O stretch
1590	strong, sharp	Aromatic C-C stretch
1653	strong, sharp	C=C stretch
1700	strong, sharp	C=O stretch
3150	short, broad	N-H stretch
3650	weak, sharp	O-H stretch

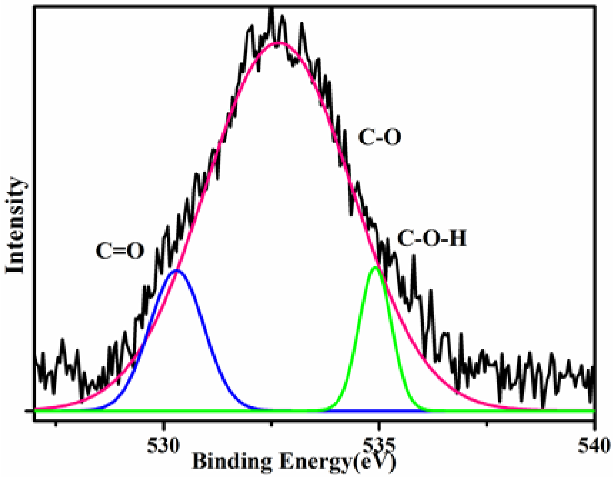

Fig. S5 O1s spectrum in the XPS analysis of **NPC-1**.

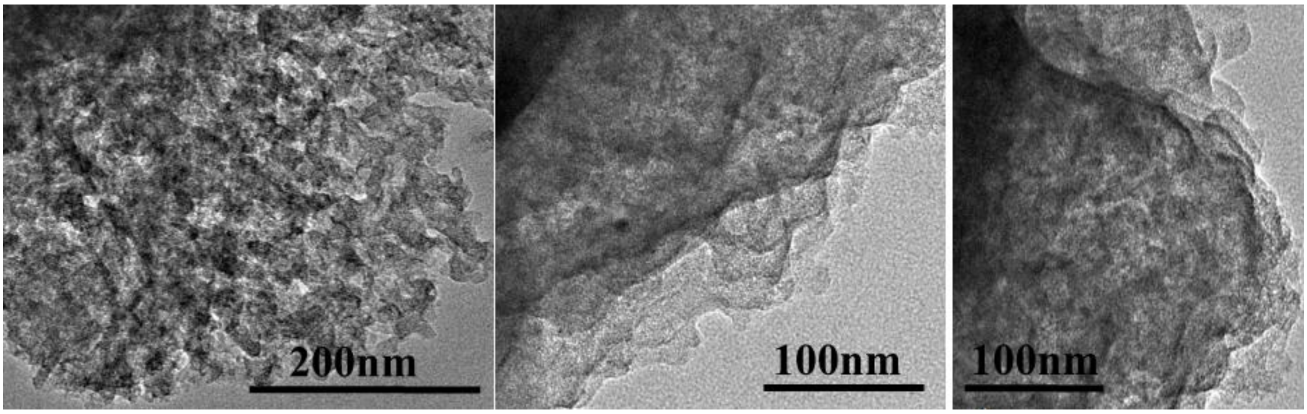

Fig. S6 TEM images at different resolutions for **NPC-1**.

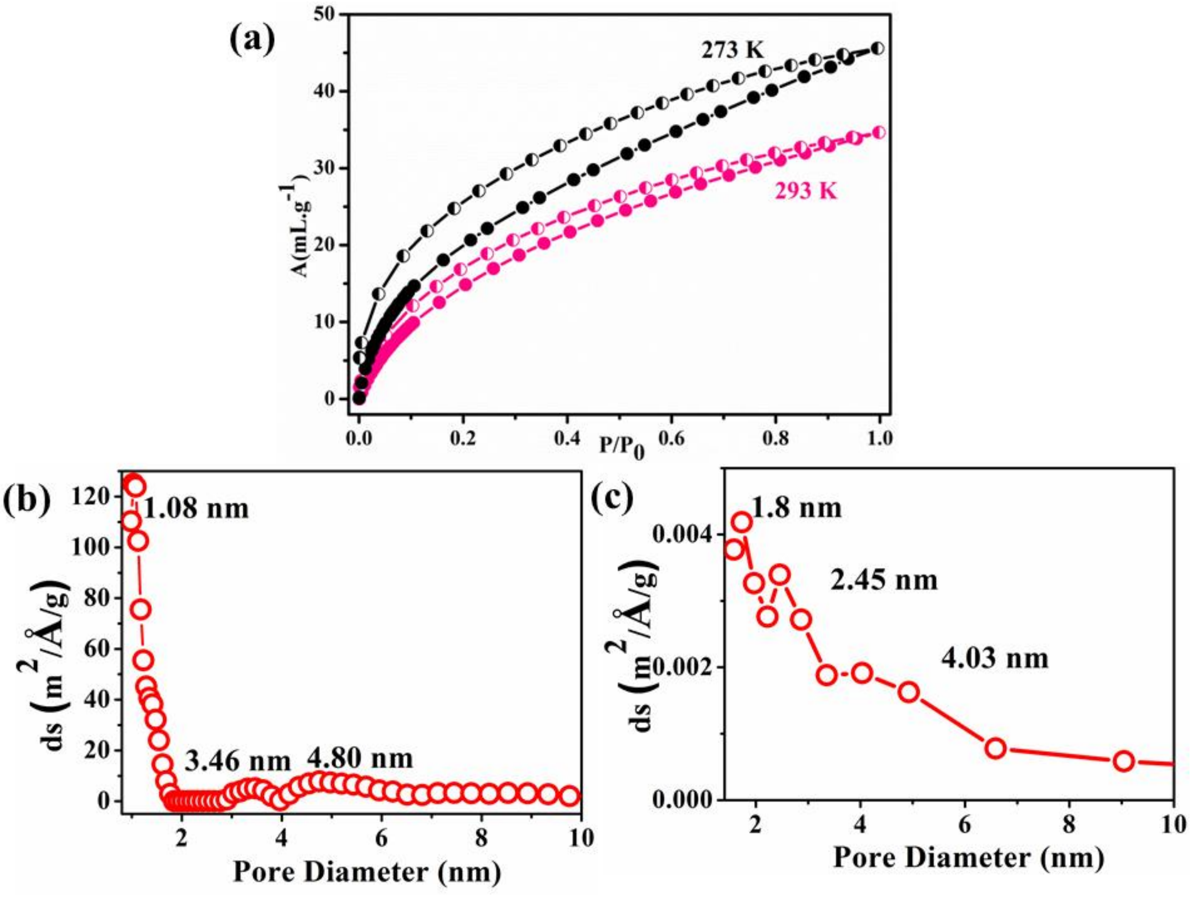

Figure S7 (a) CO_2 adsorption isotherms of **NPC-1** at 273 K (black) and 293 K (pink). Pore size distributions of **(b) NPC-1** and **(c) NCD-1**.

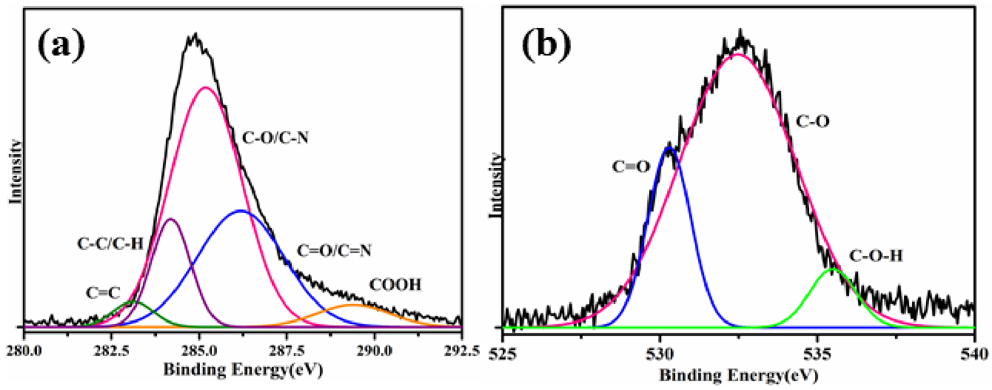

Fig. S8 (a) C1s and **(b)** O1s spectrum in the XPS analysis of **NCD-1**.

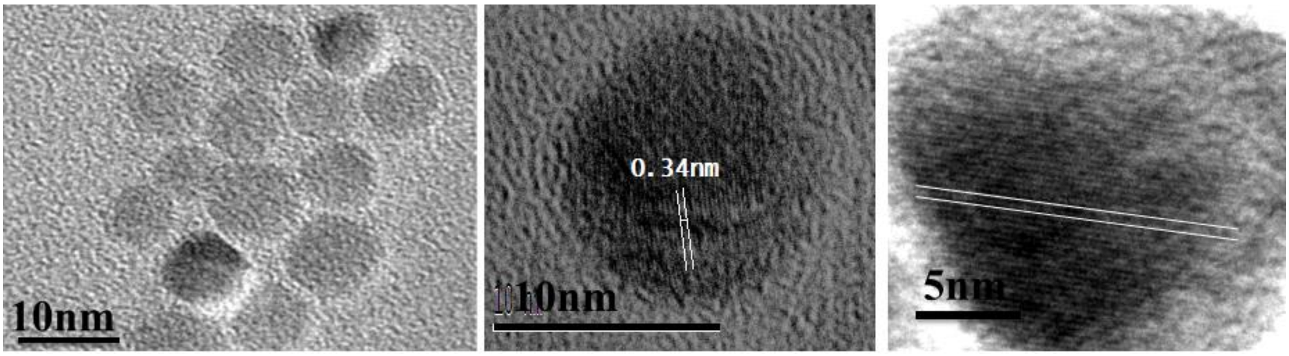

Fig. S9 TEM images at different resolutions for **NCD-1**.

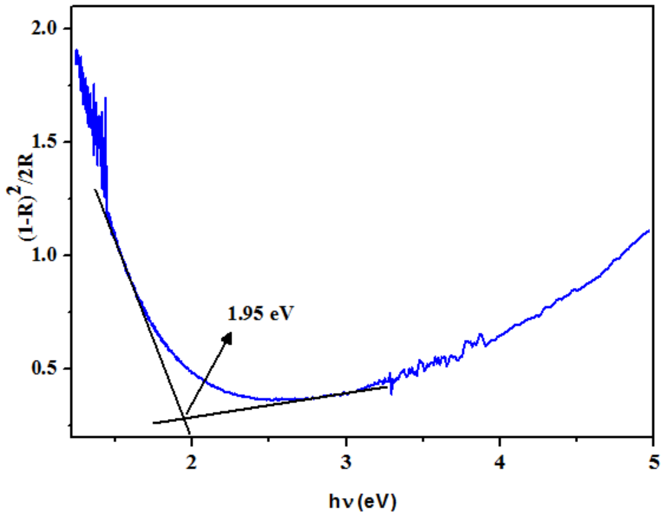

Fig. S10 Band gap calculation of **NCD-1** from Kubelka-Munk function.

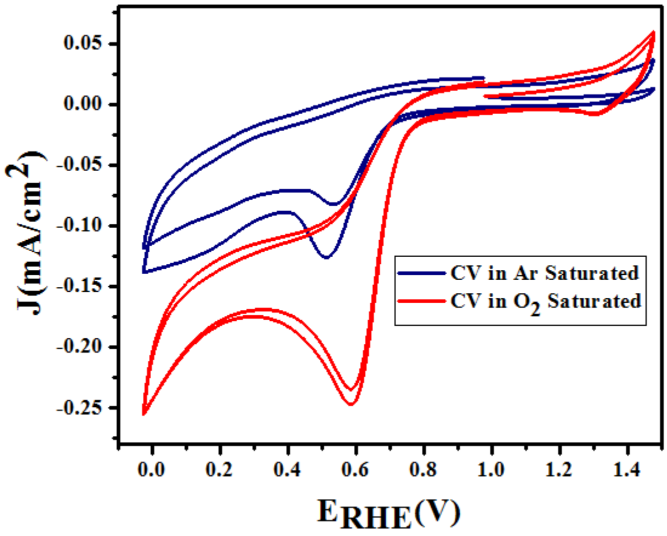

Fig. S11 CV of **NCD-1**.

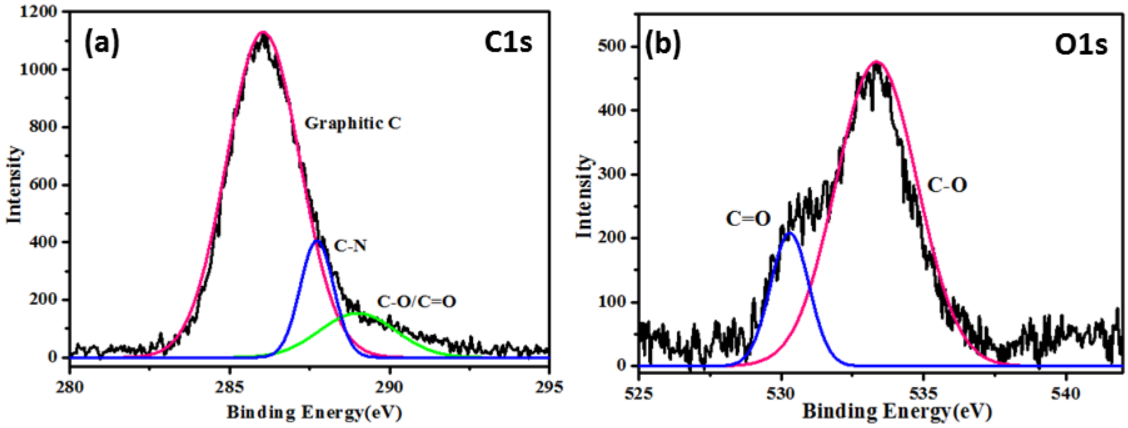

Fig. S12 (a) C1s spectrum of **Co@CN** **(b)** O1s spectrum of **Co@CN**.

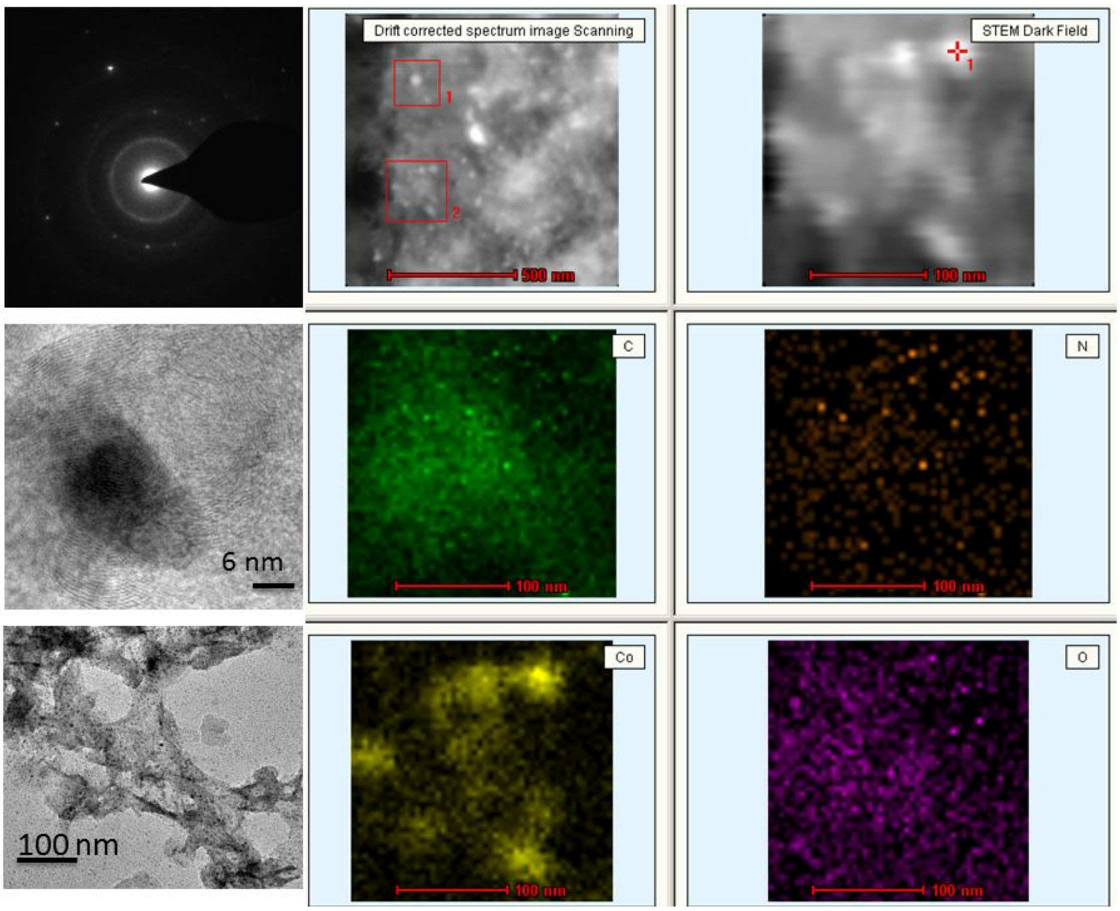

Fig. S13 Electron diffraction pattern, TEM images and colour mapping of **Co@CN**.

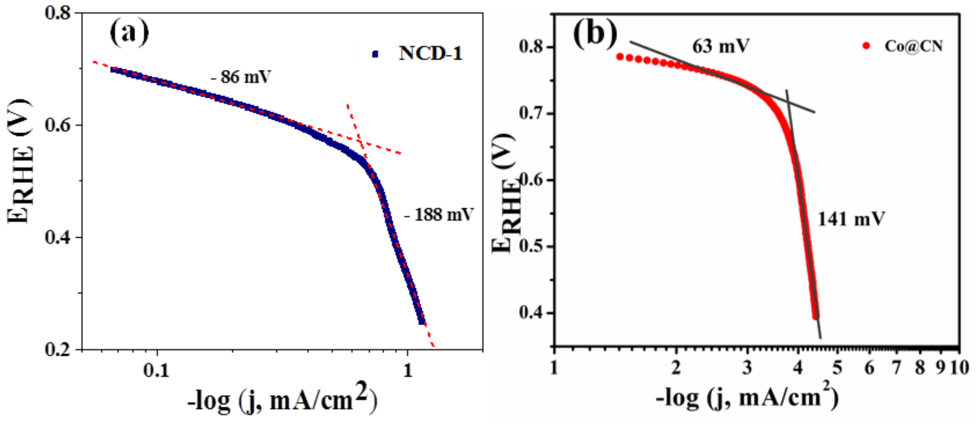

Fig. S14 Tafel plots for **(a) NCD-1** and **(b) Co@CN**.

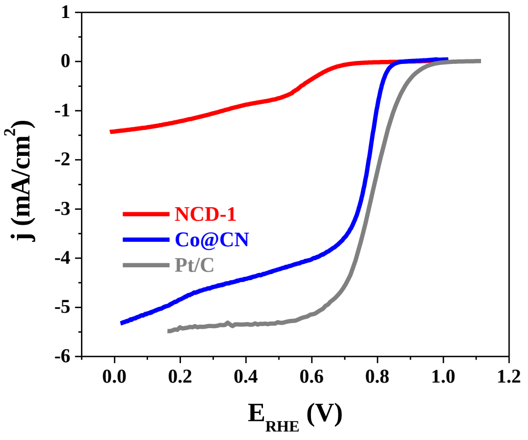

Fig. S15 Comparison of ORR activity of **Co@CN** with Pt/C.

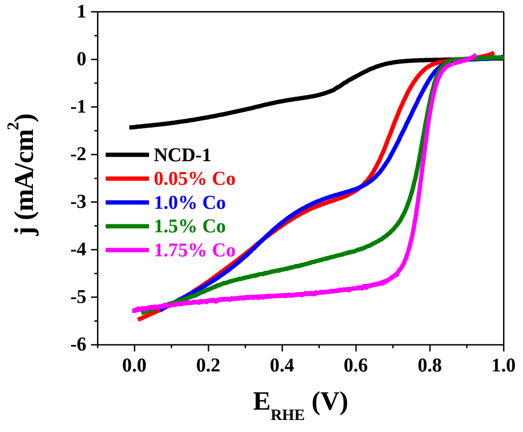

Fig. S16 ORR voltammograms recorded at 5 mV/s with **Co@CN** at different Co residues with 1600 rpm.

We examined the ORR activity of the catalyst using different concentrations of Co metal residues. As shown in **Fig. S16**, the amount 1.75 wt% Co could not improve the activity over that at 1.5wt%. There is only a noticeable change in diffusion currents.

Koutecky Levich Equation:

The kinetic parameters can be calculated on the basis of Koutecky-Levich equations:

$$\frac{1}{j} = \frac{1}{j_L} + \frac{1}{j_K} = \frac{1}{B\omega^{1/2}} + \frac{1}{j_K}$$

$B = 0.62nFC_0(D_0)^{2/3}\square^{-1/6}$

$j_K = nFkC_0$

where j_K and j_L are the kinetic and diffusion-limiting current densities, ω is the angular velocity in rad s^{-1}, n is the number of the transferred electrons, C_0 (1.26×10^{-6} mol cc^{-1}) and D_0 (1.93×10^{-5} cc s^{-1}) are the bulk concentration and diffusion coefficient of O_2 in electrolyte, υ (1.01×10^{-2} cm^2 s^{-1}) is the kinematic viscosity of the electrolyte, and k is the electron-transfer rate constant.[19] n and j_K can be determined from the slope and the intercept of the plots respectively.

Table S4 Comparison of ORR activity of different N doped C materials in alkaline media

Material	Onset Potential (V vs RHE)	Durability	Reference
NCD-1	0.72 V	28% decrease in *j* after 3 h at 0.58 V	
N-rich porous carbon	0.76 V	Negligible decrease in *j* after 1.1 h at 0.71 V	1
N doped mesoporous carbon	0.71 V	Not mentioned	2
N doped CNT	0.77 V	Not mentioned	3
N doped graphene	0.85 V	Not mentioned	4
N doped porous carbon	0.86 V	25% decrease in *j* after 7 h at 0.60 V	5

Table S5 Comparison of ORR activity of different Co doped N doped C materials in alkaline media

Material	**Co doping %**	**Over-potential values at -1 mA/cm^2 (V vs RHE)**	**Reference**
Co@CN	1.5 wt%	~0.8 V	
Co_3O_4/rmGO	20 wt%	~0.85 V	6
Co-N-C800	5 wt%	~0.82 V	**7**
Co-N-C900	0.68 wt%	~0.8 V	8
$MnCo_2O_4$/N-rmGO	65-80 wt% of $MnCo_2O_4$	~0.81 V	9

References:

[1] Pachfule, P.; Dhavale, V. M.; Kandambeth, S.; Kurungot, S.; Banerjee, R., *Chem. - Eur. J.*, 2013, *19*, 974–980.

[2] Silva, R.; Voiry, D.; Chhowalla, M.; Asefa, T., *J. Am. Chem. Soc.*, 2013, *135*, 7823−7826.

[3] Sharifi, T.; Hu, G.; Jia, X.; Wågberg, T., *ACS Nano*, 2012, *6*, 8904−8912.

[4] Lai, L.; Potts, J. R.; Zhan, D.; Wang, L.; Poh, C. K.; Tang, C.;Gong, H.; Shen, Z.; Lin, J.; Ruoff, R. S., *Energy Environ. Sci.*, 2012, *5*, 7936−7942.

[5] Zhang, P.; Sun, F.; Xiang, Z.; Shen, Z.; Yun, J.; Cao, D., *Energy Environ. Sci.*, 2014, *7*, 442−450.

[6] Liang, Y.; Li, Y.; Wang, H.; Zhou, J.; Wang, J.; Regier, T.; Dai, H., *Nat. Mater.*, 2014, 10, 780-786.

[7] Qian, Y.; Liu, Z.; Zhang, H.; Wu, P.; Cai, C., *ACS Appl. Mater. Interfaces.*, 2016, 8, 32875-32886.

[8] Guo, C.; Wu, Y.; Li, Z.; Liao, W.; Sun, L.; Wang, C.; Wen, B.; Li. Y., Chen, C., *Nanoscale Res. Lett.*, 2017, 12, 1-8.

[9] Liang, Y.; Wang, H.; Zhou, J.; Li, Y.; Wang, J.; Regier, T.; Dai, H.; *J. Am. Chem. Soc.*, 2012, 134, 3517-3523.

[10] Bhattacharyya, S.: Chakraborty, A.; Jayaramulu, K.; Hazra, A.; Maji, T. K.; *Chem. Commun.*, 2014, 50, 13567-13570.